The 12 February 2013 North Korean Underground Nuclear Test

by L.-F. Zhao, X.-B. Xie, W.-M. Wang, and Z.-X. Yao

Online Material: Figures of *Pn* waveform comparisons and spectral ratios; tables of *Pn* differential times and parameters for events used in the study.

INTRODUCTION

On 12 February 2013, North Korea conducted its third and the largest nuclear test to date in the China–North Korea border area. According to local news, people living in nearby Chinese cities experienced shaking from this explosion. The U.S. Geological Survey (USGS) reported the explosion was located at (41.301° N, 129.066° E) and the magnitude was M 5.1. This event trigged abundant regional seismic phases in northeast China, Korea, and Japan. Because of its large magnitude, the seismic records from this event showed better signal-to-noise ratios than those from previous two nuclear explosions. Illustrated in Figure 1 are broadband regional seismograms at station MDJ for three North Korea nuclear tests. These waveforms are highly similar, all are featured with abrupt *P*-wave arrivals, weak *Lg* phases and well-developed short-period Rayleigh waves. We collect the regional waveforms recorded on China National Digital Seismic Network (CNDSN), Global Seismic Network (GSN), and Japan F-net to investigate the 12 February 2013 North Korean nuclear test.

RELOCATION, DISCRIMINATION, AND YIELD ESTIMATION

High-Precision Location

By adopting the relative location method (e.g., Schaff and Richards, 2004; Zhang *et al.*, 2005; Wen and Long, 2010; Murphy *et al.*, 2013), and using the first North Korean nuclear test on 9 October 2006 as the master event, we calculate the origin times and locations of the 25 May 2009 and the 12 February 2013 North Korean nuclear tests (hereafter, referred as NKT1, 2, and 3) based on their *Pn* arrival-time differences. High-quality seismograms are selected from 57 regional seismic stations (including 5 CNDSN stations, 4 GSN stations, and 48 F-net stations), with their locations shown in Figure 2a and station parameters listed in Ⓔ Table S1 in the electronic supplement. Illustrated in Ⓔ Figure S1 (in the electronic supplement) are selected *Pn* waveforms from vertical component seismograms. In order to calculate differential times (Schaff and Richards, 2004), the *Pn* waveforms are band-pass filtered between 2.0 and 10.0 Hz and sampled by a 2 s time window starting from the *Pn* first arrival. Then the cross correlation are applied to the windowed waveforms to obtain 100 *Pn* differential travel times, as shown in Ⓔ Table S1 (in the electronic supplement).

Detonated within very close proximity, the observed seismograms from these North Korean nuclear tests are very similar at a given station. Given that the instrument and site response are the same, and propagation paths are nearly the same, we attribute the differential travel times to their relative locations, and detailed source parameters and near-source structures (e.g., *Pn* velocity beneath the test site), the burial depths, and the origin times. Because of the trade-off between burial depth and origin time, we only include origin time in calculations. Finally, we create a model with seven parameters, that is, the longitudes and latitudes of NKT2 and NKT3, the *Pn* velocity beneath the test site, and two origin times, to fit the observed *Pn* differential travel times. Because the stations are unevenly distributed azimuthally, we group the data into 20° azimuthal bins and set up a weighting function to balance their contributions. The best-fit model parameters are listed in Table 1, and shown in Figure 2b. The epicenters of NKT2 and NKT3 are (41.2936 ± 0.0003° N, 129.0770 ± 0.0006° E) and (41.2923 ± 0.0004° N, 129.0727 ± 0.0006° E], approximately 2.7 and 3.0 km away from the NKT1. The NKT3 is about 125 m south and 360 m west of the NKT2. Based on the error ellipses, the geographic precision of the relocation is 52 m. The revised origin times for NKT2 and NKT3 are 00:54:43.110 UTC and 02:57:51.270 UTC, respectively. The uppermost mantle *P*-wave velocity beneath the test site is estimated to be 7.98 ± 0.15 km/s, consisting with previous studies (Rapine and Ni, 2003; Wang *et al.*, 2003; Hearn *et al.*, 2004; Liang *et al.*, 2004; Pei *et al.*, 2007; Zhao *et al.*, 2012).

Discrimination Based on Network *P/S* Spectral Ratios

Because the explosion is an inefficient *S*-wave source, the *P*/*S*-type spectral ratios of regional phases, that is, *Pg*/*Lg*, *Pn*/*Lg*, and *Pn*/*Sn*, are widely used in explosion event discrimination (e.g., Taylor *et al.*, 1989; Walter *et al.*, 1995; Xie, 2002; Fisk, 2006; Richards and Kim, 2007; Zhao *et al.*, 2008). For the North Korean nuclear explosions and a group of nearby earthquakes, we first set proper time windows for selected phases and calculate their Fourier spectra from

 doi: 10.1785/0220130103

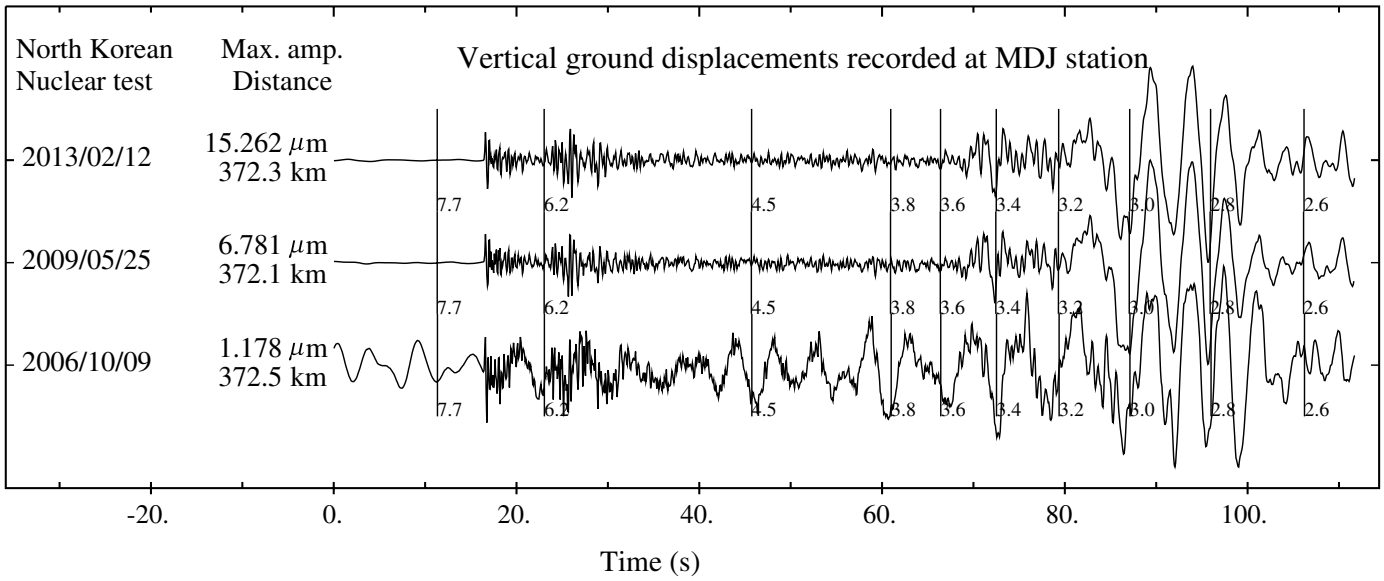

▲ **Figure 1.** Seismograms recorded on MDJ from three North Korean nuclear tests in 2013, 2009, and 2006. Illustrated are normalized vertical displacements. The event date, maximum amplitudes, and epicenter distances are listed on the left. Marks on the waveforms indicate apparent group velocities. Note that the waveforms show similar features and display clear impulsive *P*-wave onset, relatively weak *Lg* phases, and 3–5 s period Rayleigh waves.

the vertical-displacement waveforms on stations with pure continental paths (Zhao *et al.*, 2008). After distance corrections (Hartse *et al.*, 1997; Zhao *et al.*, 2008) and eliminating the data with signal-to-noise ratios lower than 1.8, we calculate their P/S spectral ratios at individual stations followed by their network averages. Ⓔ Figure S2 in the electronic supplement material gives observations at individual stations along with network averages and standard deviations. In principle, the data from individual stations show scatters while network averages effectively reduce scatters and are more reliable. Illustrated in Figure 3a–c are the Pg/Lg, Pn/Lg, and Pn/Sn ratios, respectively. In all cases, explosion and earthquake populations are fully discriminated at frequencies above 2.0 Hz, indicating an explosion within this magnitude range detonated in China–North Korea border area can be determined by a regional network without ambiguity. The network averaged P/S ratios appear to depend on the event sizes with larger event show slightly higher ratio. This phenomenon may be related to the *P*- and *S*-wave excitation mechanisms for explosion sources and depth dependence (e.g., Fisk 2006; Murphy *et al.*, 2008).

Body-Wave Magnitude $m_b(Lg)$ and Yield Estimation

Figure 4a shows a regional seismic network composed of 11 stations, which has been used for investigating the source sizes of the NKT1 and NKT2 (Zhao *et al.*, 2008, 2012). Here, we use a regional dataset (685 broadband waveforms from 98 regional events between December 1995 and February 2013, listed in Ⓔ Table S2 in the electronic supplement) and a broadband attenuation model (Zhao *et al.*, 2010) to

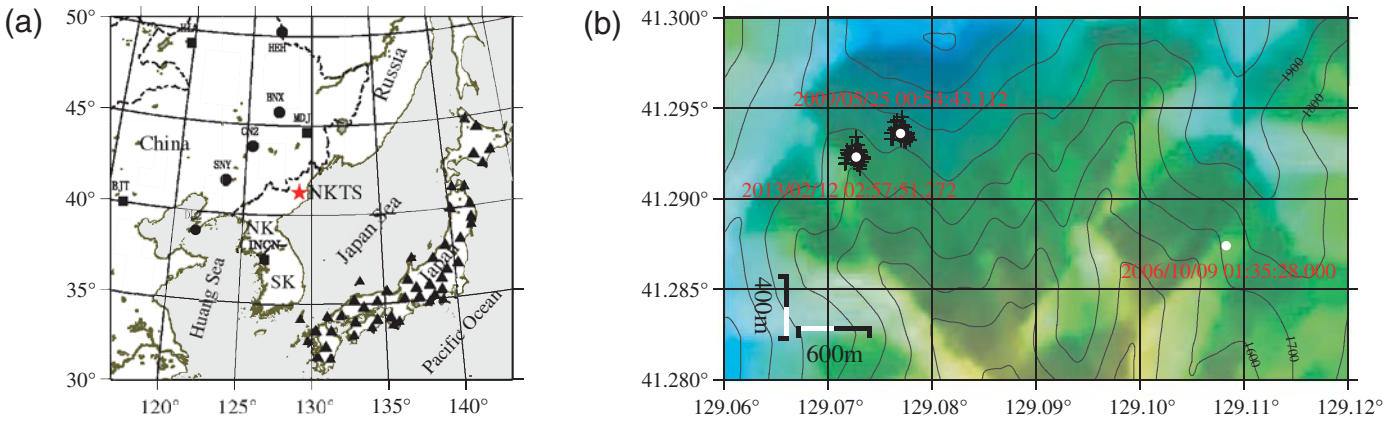

▲ **Figure 2.** (a) Map showing the locations of the North Korea test site (red star), and CNDSN (solid circles), GSN (solid squares), and F-net (triangles) stations used for relocation. (b) The topography and the locations of three North Korean nuclear tests.

Table 1
Location and Time of North Korean Nuclear Tests

NK Nuclear Test	Data (yyyy/mm/dd)	Latitude (°N)	Longitude (°E)	Origin Time (hh:mm:ss)
2006	2006/10/09	41.2874*	129.1083*	01:35:28.000†
2009	2009/05/25	41.2936	129.0770	00:54:43.110
2013	2013/02/12	41.2923	129.0727	02:57:51.270

*From satellite images (Wen and Long, 2010).
†From USGS (Wen and Long, 2010).

calibrate the regional network and use it to obtain the *Lg*-wave magnitude $m_b(Lg) = 4.91 \pm 0.22$ for NKT3.

To estimate the yield from the magnitude at an uncalibrated test site such as the North Korea test site, the empirical relations from calibrated regions may be adopted based on certain assumptions. Shown in Figure 4b are $m_b(Lg)$-yield relations for Nevada test site (NTS; Nuttli, 1986), Novaya Zemlya (Bowers *et al.*, 2001), and East Kazakhstan (Ringdal *et al.*, 1992; Murphy, 1996). For comparison, also shown in Figure 4b are three chemical explosions with known yields (Richards and Kim, 2007; Zhao *et al.*, 2012). The reported yield is the weight of ammonium nitrate explosive used in these chemical explosions (X. K. Zhang, personal comm., 2013). Because the ammonium nitrate explosive is less powerful than the trinitrotoluene (TNT), we roughly assume that 1 ton ammonium nitrate explosive equals to 0.5 ton of TNT equivalent. From the Non-Proliferation Experiment it is known that chemical explosions are more efficient at generating seismic signals by about a factor of 2 compared to nuclear explosions, if both are counted with their TNT equivalents (Denny *et al.*, 1996). After these conversions, the yields of these chemical explosions are shown in Figure 4b (refer to Zhao *et al.*, 2012). For an explosion of magnitude 4.91, these empirical relations are rather close, resulting in yields 4.04, 7.47, and 8.34 kt for NKT3 (solid line in Fig. 4b). Comparing the regional geology and upper mantle *Pn* velocity near North Korea test site with those in East Kazakhstan, Novaya Zemlya, and NTS, Zhao *et al.* (2008, 2012) preferred the fully coupled hard-rock site equation by Bowers *et al.* (2001). Using this relationship, the yield estimated for NKT3 is 7.47 kt. This value is based on the scaled depth. However, if the NKT3 is strongly overburied, the yield may be underestimated. As a comparison, the dashed lines in Figure 4b illustrate the magnitudes of NKT1 and NKT2.

DISCUSSIONS AND CONCLUSION

Based on broadband regional seismic data recorded in China, South Korea, and Japan, we investigate the location, *P*/*S* spectral ratio based discrimination, *Lg*-wave magnitude and the yield of the 12 February 2013 North Korean nuclear test. The locations and origin times of NKT2 and NKT3 are strongly dependent upon the accuracy of the reported time and location of NKT1 (Wen and Long, 2010). Because of the different datasets used, there remain minor biases between locations reported here and those from Wen and Long (2010) and Zhang and Wen (2013). The *P*/*S*-type spectral ratios are powerful discriminants to separate explosions from earthquakes. Based on single station data, Richards and Kim (2007) calculated the *Pg*/*Lg* spectral ratios for NKT1, four chemical explosions and selected earthquakes near the North Korean test site. The spectral ratios overlapped significantly under 7 Hz but were fairly well separated at 9 Hz and above. By adopting the network averages, Zhao *et al.* (2008) found that *P*/*S* spectral ratios can effectively separate NKT1 from nearby earthquakes

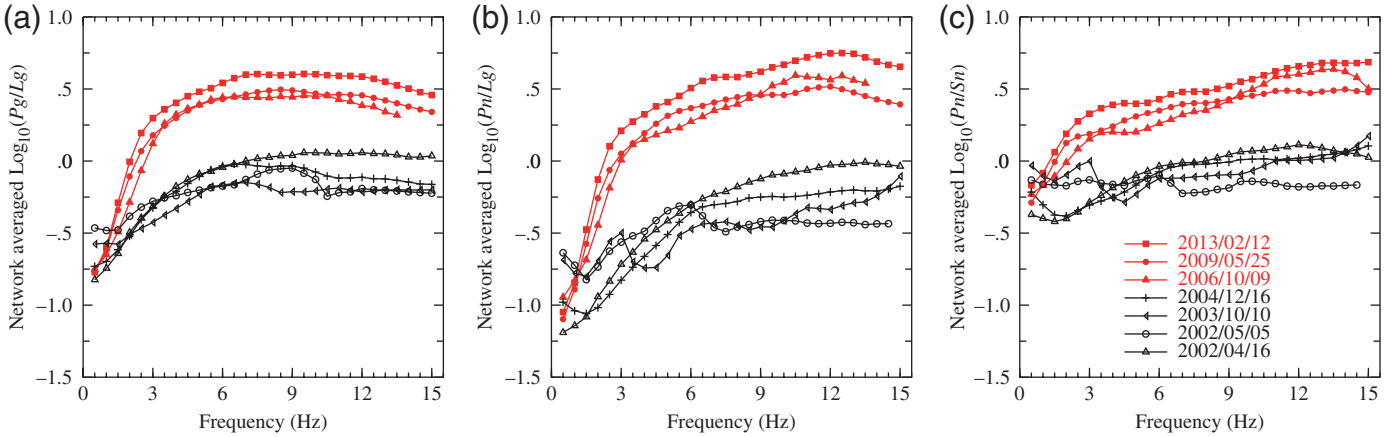

▲ **Figure 3.** The network-averaged spectral ratios for (a) *Pg*/*Lg*, (b) *Pn*/*Lg*, and (c) *Pn*/*Sn* from 7 regional events including three North Korean nuclear explosions and four nearby earthquakes (parameters are listed in Ⓔ Table S2 in the electronic supplement).

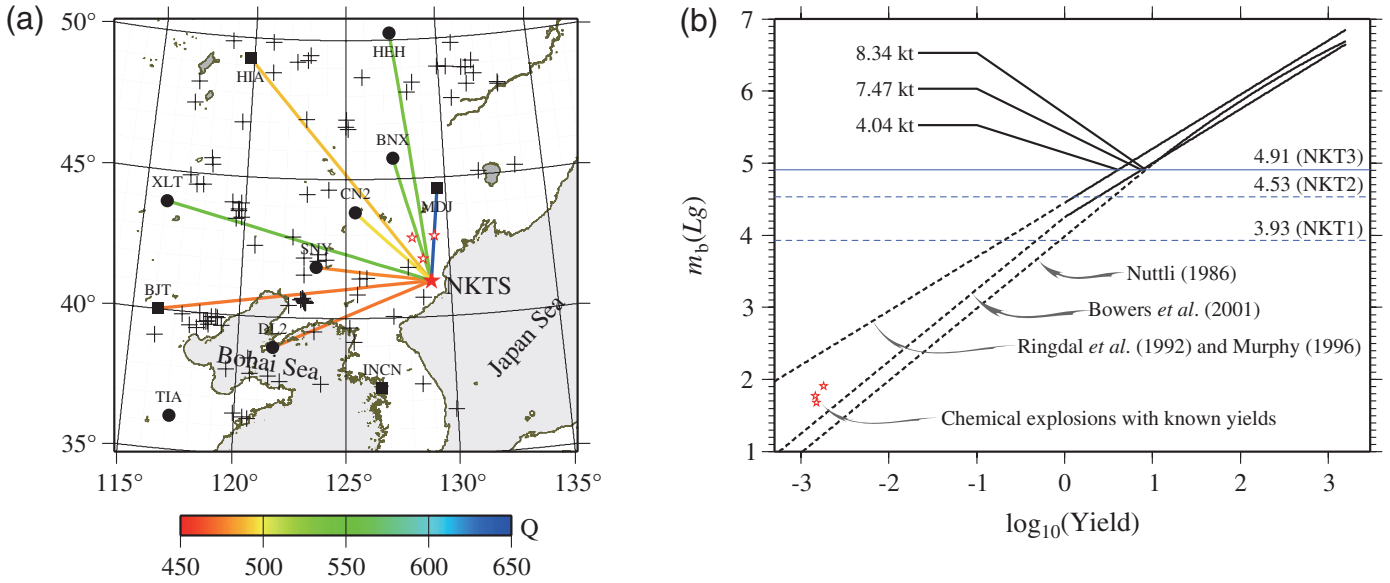

▲ **Figure 4.** (a) Map showing locations of the North Korea test site (solid red star), and CNDSN (solid circles), and GSN (solid squares) stations used for magnitude calculation and yield estimation. Also illustrated in the figure are epicenters of earthquakes (crosses) occurred between December 1995 and February 2013, and three chemical explosions (open red stars) with known yields. (b) Empirical magnitude–yield relations, where sections supported by observations are illustrated in solid lines, while the dashed lines are extrapolations. The horizontal solid line and two dashed lines indicate the estimated $m_b(Lg)$ values, 4.91, 4.53, and 3.93 for NKT3, NKT2, and NKT1, respectively. Also illustrated are three chemical explosions with known yields (stars).

at frequencies above 2 Hz. In this paper, the similar technique is tested to other North Korean nuclear tests (Fig. 3). The result confirms complete separation of explosion and earthquake populations above 2 Hz, indicating explosions similar to North Korean nuclear tests detonated in this region have good opportunity to be discriminated by a regional network. Considering the uncertainties of the source depth, the yield estimation for NKT3 is preliminary.

ACKNOWLEDGMENTS

We thank T. Lay for many discussions on this work. Both the editor and an anonymous reviewer are appreciated for their constructive comments that greatly improved this manuscript. This research was supported by the National Natural Science Foundation of China (Grants 41174048 and 40974029). X.-B. X. wishes to thank AFRL for support under Grant FA9453-11-C-0234. Waveforms recorded at the CNDSN, GSN, and F-net stations used in this study are collected from the China Earthquake Network Center (CENC), the Data Management Centre of China National Seismic Network at the Institute of Geophysics, the China Earthquake Administration (Zheng *et al.*, 2010), the Incorporated Research Institutions for Seismology Data Management Center (IRIS DMC) at www.iris.edu (last accessed April 2013), and the National research Institute for Earth science and Disaster prevention (NIED) at http://www.fnet.bosai.go.jp (last accessed April 2013). The source parameters of three chemical explosions were provided by the Geophysical Exploration Center of China Earthquake Administration (GECCEA). Some figures were created using the GMT (Wessel and Smith, 1998).

REFERENCES

Bowers, D., P. D. Marshall, and A. Douglas (2001). The level of deterrence provided by data from the SPITS seismometer array to possible violations of the comprehensive test ban in the Novaya Zemlya region, *Geophys. J. Int.* **146,** 425–438.

Denny, M., P. Goldstein, K. Mayeda, and W. Walter (1996). Seismic results from DOE's non-proliferation experiment: A comparison of chemical and nuclear xplosions, in *Monitoring a Comprehensive Test Ban Treaty*, E. S. Husebye and A. M. Dainty (Editors), Kluwer Academic Publishers, Dordrecht, 355–364.

Fisk, M. D. (2006). Source spectral modeling of regional *P*/*S* discriminants at nuclear test sites in China and the former Soviet Union, *Bull. Seismol. Soc. Am.* **96,** 2348–2367, doi: 10.1785/0120060023.

Hartse, H. E., S. R. Taylor, W. S. Scott, and G. E. Randall (1997). A preliminary study of regional seismic discrimination in central Asia with emphasis in western China, *Bull. Seismol. Soc. Am.* **87,** 551–568.

Hearn, T. M., S. Wang, J. F. Ni, Z. Xu, Y. Yu, and X. Zhang (2004). Uppermost mantle velocities beneath China and surrounding regions, *J. Geophys. Res.* **102,** no. B11301, doi 10.1029/2003JB002874.

Liang, C. T., X. Song, and J. L. Huang (2004). Tomographic inversion of *Pn* travel times in China, *J. Geophys. Res.* **109,** no. B11304, doi 10.1029/2003JB002789.

Murphy, J. R. (1996). Type of seismic events and their source descriptions, in *Monitoring a Comprehensive Test Ban Treaty*, E. S. Husebye and A. M. Dainty (Editors), Kluwer Academic Publishers, Dordrecht/Boston/London, 225–245.

Murphy, J. R., B. W. Barker, D. D. Sultanov, and O. P. Kuznetsov (2008). *S*-wave generation by underground explosions: Implications from

observed frequency-dependent source scaling, *Bull. Seismol. Soc. Am.* **99,** 809–829, doi: 10.1785/0120080126.
Murphy, J. R., J. L. Stevens, B. C. Kohl, and T. J. Bennett (2013). Advanced seismic analyses of the source characteristics of the 2006 and 2009 North Korean nuclear tests, *Bull. Seismol. Soc. Am.* **103,** 1640–1661, doi: 10.1785/0120120194.
Nuttli, O. W. (1986). *Lg* magnitudes of selected East Kazakhstan underground explosions, *Bull. Seismol. Soc. Am.* **76,** 1241–1251.
Pei, S. P., J. M. Zhao, Y. S. Sun, Z. H. Xu, S. Y. Wang, H. B. Liu, C. A. Rowe, M. N. Toksöz, and X. Gao (2007). Upper mantle seismic velocities and anisotropy in China determined through *Pn* and *Sn* tomography, *J. Geophys. Res.* **112,** no. B05312, doi: 10.1029/2006JB004409.
Rapine, R. R., and J. F. Ni (2003). Propagation characteristics of *Sn* and *Lg* in Northeastern China and Mongolia, *Bull. Seismol. Soc. Am.* **93,** 939–945.
Richards, P. G., and W.-Y. Kim (2007). Seismic signature, *Nat. Phys.* **3,** 4–6.
Ringdal, F., P. D. Marshall, and R. W. Alewine (1992). Seismic yield determination of Soviet underground explosions at the Shagan River test site, *Geophys. J. Int.* **109,** 65–77.
Schaff, D. P., and P. G. Richards (2004). Repeating seismic events in China, *Science* **303,** 1176–1178, doi: 10.1126/science.1093422.
Taylor, S. R., M. D. Denny, E. S. Vergino, and R. E. Glaser (1989). Regional discrimination between NTS explosions and western U.S. earthquakes, *Bull. Seismol. Soc. Am.* **79,** 1142–1176.
Walter, W. R., K. Mayeda, and H. J. Patton (1995). Phase and spectral ratio discrimination between NTS earthquakes and explosions Part 1: Empirical observations, *Bull. Seismol. Soc. Am.* **85,** 1050–1067.
Wang, S., Z. Xu, and S. Pei (2003). Velocity structure of uppermost mantle beneath North China from *Pn* tomography and its implications, *Sci. China Earth Sci.* **46,** 130–140, doi: 10.1360/03dz0010.
Wen, L., and H. Long (2010). High-precision Location of North Korea's 2009 Nuclear Test, *Seismol. Res. Lett.* **81,** 26–29, doi: 10.1785/gssrl.81.1.26.
Wessel, P., and W. Smith (1998). New, improved version of the generic mapping tools released, *Eos Trans. AGU* **79,** 579.
Xie, J. (2002). Source scaling of *Pn* and *Lg* spectra and their ratios from explosions in central Asia: Implications for the identification of small seismic events at regional distances, *J. Geophys. Res.* **107,** no. B7, doi: 10.1029/2001JB000509.
Zhang, J., X. Song, Y. Li, P. G. Richards, X. Sun, and F. Waldhauser (2005). Inner core differential motion confirmed by earthquake waveform doublets, *Science* **309,** 1357–1360.
Zhang, M., and L. Wen (2013). High-precision location and yield of North Korea's 2013 nuclear test, *Geophys. Res. Lett.* **40,** 2941–2946, doi: 10.1029/grl.50607.
Zhao, L. F., X. B. Xie, W. M. Wang, and Z. X. Yao (2008). Regional seismic characteristics of the 9 October 2006 North Korean nuclear test, *Bull. Seismol. Soc. Am.* **98,** 2571–2589, doi: 10.1785/0120080128.
Zhao, L. F., X. B. Xie, W. M. Wang, and Z. X. Yao (2012). Yield estimation of the 25 May 2009 North Korean nuclear explosion, *Bull. Seismol. Soc. Am.* **102,** 467–478, doi: 10.1785/0120110163.
Zhao, L. F., X. B. Xie, W. M. Wang, J. H. Zhang, and Z. X. Yao (2010). Seismic *Lg*-wave *Q* tomography in and around Northeast China, *J. Geophys. Res.* **115,** no. B08307, doi: 10.1029/2009JB007157.
Zheng, X. F., Z. X. Yao, J. H. Liang, and J. Zheng (2010). The role played and opportunities provided by IGP DMC of China National Seismic Network in Wenchuan earthquake disaster relief and researches, *Bull. Seismol. Soc. Am.* **100,** 2866–2872, doi: 10.1785/0120090257.

L.-F. Zhao
Z.-X. Yao
Key Laboratory of the Earth's Deep Interior
Institute of Geology and Geophysics
Chinese Academy of Sciences
19 Beituchengxilu
Chaoyang district
Beijing 100029, China
zhaolf@mail.iggcas.ac.cn

X.-B. Xie
Institute of Geophysics and Planetary Physics
University of California at Santa Cruz
1156 High Street
Santa Cruz, California 95064 U.S.A.
xxie@ucsc.edu

W.-M. Wang
Key Laboratory of Continental Collision and Plateau Uplift
Institute of Tibetan Plateau Research
Chinese Academy of Sciences
18 Shuangqinglu Road
Haidian District
Beijing 100085, China
wangwm@itpcas.ac.cn